

Dependence of Electrical Resistivity on Plastic Deformation in Copper-Aluminum Alloy $\text{Cu}_{0.975}\text{Al}_{0.025}$

J.G. Miranda Ramos¹, E. Medrano Atencio¹, M. Quiroga Agurto¹, and F.A. Reyes Navarro^{1*}

¹ Laboratorio de Cristales Reales y Aleaciones Metálicas (LABCRAM), Facultad de Ciencias Físicas, Universidad Nacional Mayor de San Marcos (UNMSM), Calle Germán Amézaga N° 375, Lima, Peru.

Abstract

We measure changes of electrical resistivity after a plastic deformation. We supposed that the changes are due to a large density of dislocation present in the polycrystalline samples; therefore, we also measure the amount of dislocations after the plastic deformation. Thus, for our aim, we elaborated copper-aluminum alloys $\text{Cu}_{0.975}\text{Al}_{0.025}$; afterwards, with them, we fabricated metallographic specimens, which were submitted to traction subsequently. We measured the electrical resistivity before and after the traction. The obtained results are discussed in a theoretical framework of dislocations.

Introduction

Interest to know what happens inside a metal began in 1827, when G. S. Ohm discovered his famous law. Three years later, P. Drude presented a model on metals, which gave satisfactory answers to some issues such as electrical resistivity⁽¹⁾. Later, in 1908, at the University of Leyden (Netherlands), investigating how impurities influence in electrical resistivity (which could be measured relatively easily at low temperatures), K. Onnes found zero electrical resistivity, i.e., discovered superconductivity. Also, in 1927, A. Sommerfeld introduced its model on metals, which is based on the quantum mechanical theory (Pauli Exclusion Principle); this model responded satisfactorily to more questions about the electrical resistivity⁽¹⁾. Other relevant works concerning study of the dependence of electrical resistivity on dislocations in single and polycrystals are as follows⁽²⁻⁸⁾: J. S. Koehler (1949), J. K. Mackenzie (1950), R. Landauer (1951), D. L. Dexter (1952), C. Macchioni *et al.* (1982), R. P. Gupta (1987), M. Niewczas (2014), and Q. Bian & M. Niewczas (2016).

The motivation for this study is to determine the influence of the irreversible movement of dislocations (plastic deformation) on the electrical resistivity, because it is important to know the behavior of electrons when the crystal lattice is under strain⁽⁹⁾. More specifically, this paper aims to demonstrate experimentally the dependence of the electrical resistivity on the real crystal structure (dislocations). In the next section, we give the

physical properties of copper, aluminum, and copper-aluminum alloy. In the antepenultimate section, we make a description of the experimental work made; we show how procedures were performed, e.g., computing of the density of the sample, its melting and polishing, determination of the dislocation density (as observed in the metallographic optical microscope), electrical resistivity measurement before and after pulling the test specimen. In the penultimate section, we present sequentially the results in tables, according to the data collected; also, we plot the electrical resistivity as a function of plastic deformation and dislocation density, respectively. We furthermore make a discussion of the curves obtained. In last section, we present the conclusions of this work.

Theoretical framework

The most important properties of copper are good electrical and thermal conductivity, as well as high plasticity and ability to form alloys; all of which allow a wide range of industrial applications⁽¹⁰⁾. Specifically, copper has a face-centered cubic crystal structure, with lattice parameter $a=0.364$ nm; density 8.93 g/cm³; melting temperature 1083°C ; and boiling temperature 2360°C . Also, after the processes of lamination and annealing, copper has plasticity between 30-35%⁽¹⁰⁾. As a result of the high plasticity, copper easily deforms when it is in hot and cold states. Furthermore, as a consequence of cold deformation, the mechanical strength of copper can grow up to 700 MN/m²; however, its plasticity decreases simultaneously up to 1-3%. The electrical conductivity

of copper, at 20°C in quenched state, is $5.8 \times 10^5 \Omega^{-1} \text{cm}^{-1}$.

With respect to impurities in the copper, they can be classified by the character of the interaction⁽¹¹⁾: 1) Impurities forming solid solutions (nickel, zirconium, antimony, tin, arsenic, iron, phosphorus). These impurities improve the mechanical properties but decrease abruptly the electrical and thermal conductivity of copper (especially antimony and arsenic). Consequently, for current conductors it is utilized M0 and M1 copper, which contain no more than 0.0002% of Sb and 0.0002% of As, too. 2) Lead and bismuth impurities, which are detrimental for copper and its alloys; even in small amounts (hundredths or thousandths of a percentage point), they drastically reduce the ductility of copper at high temperatures. 3) Oxygen and sulfur impurities forming with copper brittle chemical compounds, Cu_2O and Cu_2S , which are distributed by the intergranular boundaries. Sulfur improves copper produced by cutting. These impurities do not influence practically on the electrical conductivity.

With regard to aluminum, the most important properties, which determine a wide range of applications, are as follows: boiling temperature 2500°C, melting temperature 658°C, face-centered cubic crystal structure with lattice parameter $a=0.4049 \text{ nm}$, density 2.72 g/cm^3 , and high electrical and thermal conductivity⁽¹¹⁾. Pure aluminum is resistant to corrosion, what is explained by the formation on the surface of a compact and passivating film of aluminum oxide (Al_2O_3)⁽¹²⁾. The purer aluminum, the higher the resistivity to corrosion and the greater electrical conductivity; also, pure aluminum is easily laminated into thin foils, pressed and printed. Main impurities in aluminum are iron and silicon; they increase the aluminum's hardness, but simultaneously decrease its plasticity and corrosion resistance, too. Deformed and annealed aluminum has high plasticity (35-40%) and low mechanical resistance. The strength and hardness of aluminum can be increased by cold working (strain hardening). To remove the aluminum's hardness, it must be subjected to a recrystallization annealing temperature between 300 and 360°C.

Furthermore, regarding the copper-aluminum alloy, its phase diagram describes its structural regularities (see⁽¹³⁾). In general, alloys' phase diagrams graphically show the alloys' phase composition and structure as a function of temperature and weight percent; those diagrams are constructed under

conditions of thermodynamic equilibrium. The free energy of the system must remain unchanged, what is only achieved at very slow cooling rates. Specifically, the copper-aluminum's phase diagram has numerous intermetallic phases⁽¹³⁾. For example, up to 9.5% Al, at 565°C, copper is characterized by a solid solution; but with 8.5% Al the alloy is an aluminum bronze having the α phase. Because of segregation and solidification, and cooling in non-equilibrium, the melted alloys from 8.5 to 9.5% Al are characterized by high concentrations of the β phase (which has an aluminum's stable content from about 8.5 % to 15% when temperature augments). The β phase the electron compound Cu_3Al having an electron concentration 3/2; it has a body-centered cubic structure ($a=0.2945 \text{ nm}$). After a cooling process, the alloy dissociates into $\alpha+\gamma_2$ by a eutectoid transformation (γ_2 is the electron compound $\text{Cu}_{32}\text{Al}_{19}$). Besides, in the corresponding diagram of phases, we can find the χ phase, which includes Cu_9Al_4 with electron concentration 21/13 (it is a compound being stable above 963°C).

Experimental method

Obtaining of the copper-aluminum alloy

Computing of the alloy components' masses

For the preparation of the samples intended for mechanical testing and electrical resistivity measurement, we use the following equation:

$$D_{\alpha} = \frac{D_{\text{Cu}}D_{\text{Al}}}{\%_{\text{Al}}D_{\text{Cu}} + \%_{\text{Cu}}D_{\text{Al}}} \quad (1)$$

where D_{α} is the density of the alloy; D_{Cu} , density of copper; and D_{Al} , density of aluminum. Therefore, by using the previous formula, we can determine the mass of the specimen by $M_{\text{sp}}=D_{\alpha}V_{\text{sp}}$, where M_{sp} and V_{sp} are, respectively, the mass and the volume of the specimen.

Casting

To melt the masses of copper and aluminum, we proceed as follows: a) we placed in the crucible the necessary amount of copper; next, we bring the flamethrower closer. When copper is almost to melt, it is added the determined amount of aluminum. b) When the alloy is in liquid state, it is poured into an ingot mold; afterwards, the solidified alloy is removed from the ingot mold and allowed to cool down to room temperature. Later, the alloy is laminated,

with a thickness of 3 mm. Lastly, we proceed to cut it with the appropriate shape and size.

Thermal treatment

In order to remove internal tensions accumulated during lamination, the obtained test specimens are subjected to a heat treatment at 360°C for two hours. Among the dimensions of the specimen there is a certain relationship, namely, the initial length L_0 satisfies $L_0 = 2.82 \sqrt{S_0}$, with S_0 the cross-sectional initial area of the specimen, which thus obtained is a standard one.

Deburring, polishing and chemical attack

Before characterizing the metallographic specimen with an optical microscope (for determining the density of dislocations), we followed the following procedure: a) we perform the elimination of the burrs through a deburring machine with three types of abrasive papers: 100, 360 and 400. In this process, the removed burrs were cleaned by the water hose connected to the deburring machine. b) For the polishing, we proceeded as follows: in the polisher pad, we put magnesium oxide (MgO) dissolved in distilled water; then, we started to rub the specimen, at the same time wash it in distilled water jets, until we get a mirror-like specimen surface. c) To make the chemical attack, which will expose the structure of the alloy, we use the following solution: 4 ml of ferric chloride ($FeCl_3$), 2 ml of hydrochloric acid (a pungent solution of hydrogen chloride, HCl, in water), 1 ml of acetic acid (CH_3COOH), and 5 drops of bromine. The chemical attack consists in rubbing the polished face of the specimen with a cotton ball soaked with the mentioned reagents. Finally, we washed with water the specimen and dried it with a tissue paper.

Tensile testing

This type of mechanical test allows to elongate the elaborated specimens; consequently deformations in them can be determined by the formula $\varepsilon = \frac{\Delta L}{L_0} 100\%$, where L_0 is the initial length before traction; L , final length after it. Regarding the tensile testing machine utilized, it consists of the following parts: 1) a hydraulic press, which is the main part of the machine, whose operation allows the specimen to elongate. 2) Fixed columns that serve to support the hydraulic press. 3) Mobile crossheads, whose displacement, caused by the piston thrust of the hydraulic press, pulls the

specimen. 4) Holding grips, which serve to hold the specimen. 5) Pressure gauge, which records changes in hydraulic press' pressure transmitted to the mobile crossheads.

Regarding the operation of the tensile testing machine, we have the following steps: 1) We placed the specimen between the holding grips and firmly fixed it with the screws of the holding grips. 2) We take care that the oil-flow control valve, in the hydraulic press, is closed, and only then we start pumping. 3) We augment gradually the stress and measure the deformation for each of the test specimens.

Determination of the dislocation density (D)

We followed three steps: 1) we placed the chemically attacked sample on the light-microscope specimen holder. 2) We focused the selected area and counted the number of dislocations in each element of the microscope eyepiece reticle. 3) We averaged the number of dislocations, and divide it by the reticle areas; the end result is given in dislocations/ m^2 .

Measurement of the electrical resistivity

We use a conventional method known as four-terminal sensing, which usually is not destructive. We utilized the usual geometry, i.e., we placed linearly the four terminals, with equal spacing. The current must pass through the two outer terminals, and the voltage must be measured in the other two terminals (another non-destructive method for arbitrary conductive samples is the Van der Pauw method)⁽¹⁴⁾. Specifically, we have calculated the alloys' electrical resistivity by using the basic formula $\rho = AV/(LI)$, where A is the cross-sectional area; L , spacing between two terminals; V , voltage; and I , current.

We must also indicate some restrictions that we have considered: a) The samples must be semi-infinite, i.e., dimensions of the samples are large when compared to the spacing between the terminals. b) To avoid injection of minority carriers in the current contacts, we polished with sandpaper the surface of the samples.

Results and discussions

The specimens obtained by melting of copper and aluminum are technically pure (Cu 99.95% and Al 99.67%), and we characterized them with a light

microscope, wherein we observe that the samples are constituted by a copper-aluminum solid solution α . We have also determined the lattice parameters: 0.362nm for the alloy, 0.3608nm for copper, and 0.4043nm for aluminum.

Table 1 shows the results for the electrical resistivity measurement, and the characterization by using the light microscope (both before plastic

deformation). Likewise, Table 2 has the results for the tensile test, electrical resistivity measurement, and the characterization by using the light microscope (all after plastic deformation).

Table 1. Before plastic deformation, average data obtained for electrical resistivity (ρ), and density of dislocations (D). Each sample was measured ten times.

Sample	1	2	3	4	5	6	7
ρ ($\mu\Omega$.cm)	4.5169	4.8734	4.8517	5.7182	5.4019	5.3736	4.3068
D (#Disl./m ² x10 ⁷)	1.592	1.500	1.080	1.248	1.648	2.372	1.516

Table 2. After plastic deformation, average data obtained for deformation (ϵ), electrical resistivity (ρ), and density of dislocations (D). Each sample was measured ten times.

Sample	1	2	3	4	5	6	7
ϵ (%)	2.16	9.69	13.03	16.15	16.27	27.13	34.45
ρ ($\mu\Omega$.cm)	4.9878	5.0123	6.2320	6.6976	5.9189	5.8386	4.9592
D(#Disl./m ² x10 ⁷)	1.720	1.464	1.168	1.892	1.468	1.524	1.608

In Figure 1, we have electrical resistivity vs. density of dislocations; this curve fits for a third-degree polynomial, $f(x) = -103.70165 + 23.54617x - 1.65231x^2 + 0.03785x^3$. We can divide Figure 1 into the following three regions: 1) Region A, from 1.1×10^7 to 1.25×10^7 Disl./m². We observe the increase of the electrical resistivity from 5.7 to $6.4\mu\Omega$ cm. Because of the onset of plastic deformation, new dislocations arise; when they interact with the electrons, the displacement of these last is obstructed⁽¹¹⁾. 2) Region B, from 1.25×10^7 to 1.65×10^7 Disl./m². We realize electrical resistivity decreased to $5.4\mu\Omega$ cm, what is due to the annihilation of some dislocations. This annihilation occurs during the continuous development of plastic deformation of the alloy, enabling the quasi-free movement of electrons⁽¹⁵⁾. 3) Region C, from 1.65×10^7 to 1.90×10^7 Disl./m². We notice the rapid increase in the electrical resistivity, what is due to the increase of dislocations at this stage of the alloy deformation. Because dislocations interact each other, forest dislocations originate as well as the hardening of the specimen until fracture; the forest dislocations make the movement of electrons more difficult⁽¹¹⁾.

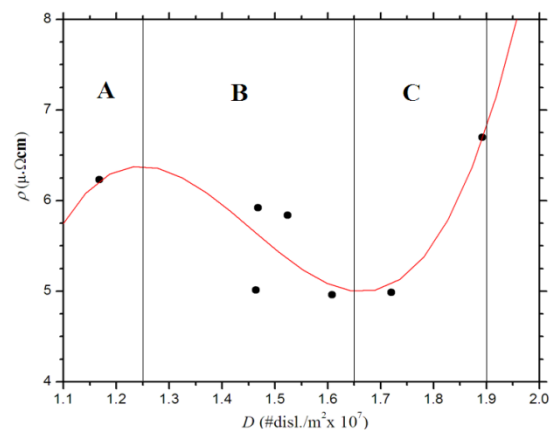


Figure1. Electrical resistivity vs. density of dislocations

In Figure 2., red curve fits for a second-degree polynomial, $f(x) = 4.43159 + 0.17676x - 0.00446x^2$, with standard deviation 0.49875; blue curve, for a third-degree polynomial, $f(x) = 18.8783 - 0.63137x + 0.036x^2 - 5.59186x^3$, with standard deviation 2.98132. To analyze Figure 2, we divide it into three regions. In region I (0-12.5% deformation), the larger plastic deformation, the larger the electrical resistivity. This link shows that the specimen's deformed crystal structure provides

certain resistance to the conduction electrons' flux; besides, this connection makes clear that aluminum impurities constitute scattering centers. In this region, we also observe diminution of the density of dislocations, due to an annihilation of dislocations. In region II, 12.5-20% deformation, the electrical resistivity and the density of dislocations augment; this occurs because the increase of dislocations in the specimens restricts the electrons' flux, i.e., an electron-dislocation interaction happens. In region III (20-30% deformation), the electrical resistivity diminishes slightly, but the density of dislocations increase. This fact can be explained as follows: the microstructures, as the density of dislocations augment, majorly form thick immobile dislocations. Likewise, there is a great stresses' concentration inducing the alloy microstructure; this way it is obtained a high potential energy of ions, which interact with the conduction electrons' flux. Consequently, the electrical resistivity diminishes.

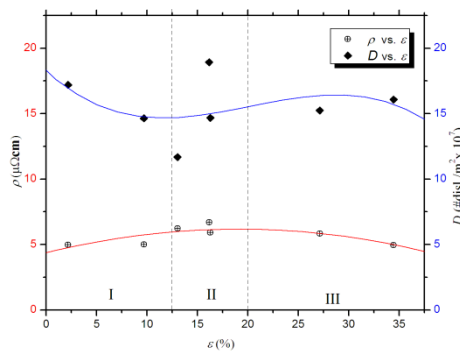


Figure 2. On the left vertical axis, we have electrical resistivity; on the right vertical axis, density of dislocations; and on the horizontal axis, plastic deformation.

Conclusions

Based on the dependence of electrical resistivity on dislocations in $\text{Cu}_{0.975}\text{Al}_{0.025}$, we conclude that the behavior of the electrical resistivity is provoked by the following facts: the presence of dislocations initially appearing, the annihilation of dislocations, and the formation of forest dislocations.

Likewise, in accordance with measurements of electrical resistivity and deformation, we can affirm that the specimen's deformed crystal structure provokes resistance to the conduction electrons' flux, what is indicative that aluminum impurities constitute scattering centers.

Acknowledgments

We thank so much M. Niewczas, from McMaster University (Canada), who provides us some references useful for this work.

References

1. Pavlov, P.V. and Jojlov, A.F. (1987). *Física del estado sólido* (Solid state physics). Mir Publishers Moscow.
2. Koehler, J.S. (1949). A calculation of the changes in the conductivity of metals produced by Cold-Work. *Phys. Rev.* **75**(1) : 106.
3. Mackenzie, J.K. and Sondheimer, E.H. (1950). The theory of the change in the conductivity of metals produced by cold work. *Phys. Rev.* **77**(2) : 26.
4. Landauer, R. (1951). Conductivity of cold worked metals. *Phys. Rev.* **82**(4) : 520.
5. Dexter, D. L. (1952). Scattering of electrons in metals by dislocations. *Phys. Rev.* **86**(5) : 760.
Dexter, D.L. (1952). Conductivity of cold-worked metals. *Phys. Rev.* **85**(5) : 936.
6. Macchioni, C., Rayne, J.A., and Bauer, C.L. (1982). Low-temperature resistivity of bulk copper- aluminum alloys. *Phys. Rev. B.* **25**(6) : 3865.
7. Gupta, R.P. (1987). Residual resistivity of defects in metals. *Phys. Rev. B.* **35**(11) : 5431.
8. Bian, Q. and Niewczas, M. (2016). Theory of magnetoresistance due to lattice dislocations in face-centred cubic metals. *Philosophical Magazine.* **96**(17) : 1832–1860.
Niewczas, M. (2014). Intermittent plastic flow of single crystals: central problems in plasticity: a review. *Materials Science and Technology,* **30**(7) : 739–757.
9. Miranda Ramos, J.G. 2006. Licentiate Thesis entitled *Resistividad eléctrica en función de la deformación plástica de la aleación de cobre con aluminio*

(Electric resistivity as a function of the plastic deformation of copper-aluminum alloy), UNMSM, Lima, Peru

10. Kuzmin, B.A., and Samojotski, A.I. (1986). *Metalurgia, metalografía y materiales de construcción* (Metallurgy, metallography and special-purpose materials). Mir Publishers, Moscow.
11. Lajtin, Y.M. (1973). *Metalografía y tratamiento térmico de los metales* (Metallography and heat treatment of metals). Mir Publishers Moscow.
12. Castillo, M.R. (2007). *El Aluminio: Aspectos generales* (Aluminum: General aspects). Universidad Bolivariana de los Trabajadores, Centro de Formación RIALCA, Venezuela. https://ubtjrialca.files.wordpress.com/2012/02/elaluminio_y_su_desarrolloactua11.pdf
13. AGH University of Science and Technology, Faculty of Non-Ferrous Metals, Cracow, Poland. 2016. <http://www.conductivity-app.org/single-article/cu-overview>
14. Heaney, M. B. 1999. Electrical conductivity and resistivity IN "Measurement, instrumentation, and sensors handbook CRCnetBase" (Section VII: Electromagnetic Variables Measurement), Ed. John G. Webster. <http://www.kelm.ftn.uns.ac.rs/literatura/si/pdf/Measurement%20Instrumentation%20Sensors.pdf>
15. Reed-Hill, R. E. 1971. *Principio de metalurgia física* (Principles of physical metallurgy). Editorial Continental S.A. México, España, Argentina, Chile.